Correlation between Particle Motion and Voronoi-Cell-Shape Fluctuations during the Compaction of Granular Matter

Steven Slotterback,[1,*] Masahiro Toiya,[1] Leonard Goff,[1] Jack F. Douglas,[2,†] and Wolfgang Losert[3,‡]

[1]*Department of Physics, and IREAP, University of Maryland, College Park, Maryland 20742, USA*
[2]*Polymers Division and Center for Theoretical and Computational Materials Science, National Institute for Standards and Technology, Gaithersburg, Maryland 20899, USA*
[3]*Department of Physics, IPST, and IREAP, University of Maryland, College Park, Maryland 20742, USA*

We track particle motions in a granular material subjected to compaction using a laser scattering-based imaging method where compaction is achieved through thermal cycling. Particle displacements in this jammed fluid correlate strongly with rearrangements of the Voronoi cells defining the local environment about the particles, similar to previous observations of Rahman on cooled liquids. Our observations provide further evidence of commonalities between particle dynamics in granular matter close to jamming and supercooled liquids.

DOI: 10.1103/PhysRevLett.101.258001   PACS numbers: 45.70.Cc, 81.05.Rm

Granular materials are strongly interacting particle systems that admit an admixture of collective particle motions, as in crystals, and random particle motions, as in simple fluids. Under flow or deformation conditions, these materials pass intermittently between a solid "jammed" state and a state of flow. When a granular material jams, the individual particles are in stable mechanical equilibrium with their local neighbors [1]. Small perturbations such as tapping [2] or shearing [3] can move the particles and lead to the evolution from one jammed state to another, generally more compact state [1,4]. Recent computational and experimental studies have demonstrated that particle motion in certain driven granular fluids [5] can have features in common with glass-forming liquids (e.g., transient particle caging and stringlike collective motion [6–9]).

One of the outstanding questions about strongly interacting particle systems is how local fluctuations in the particle environment influence the correlated motion that arises in this broad class of "fluids." The transition between caged and correlated motion states evidently reflects fluctuations in the particle environment that open up channels of particle motion, but this aspect of strongly interacting fluids remains poorly understood. Average measures of the local particle structural environment, such as the pair correlation function, provide no information about the origin of collective particle motion, and the present work focuses exclusively on these environmental fluctuations.

Following Rahman [10] in the context of cooled molecular fluids, it is natural to investigate the *dynamical* properties of the Voronoi cells uniquely defining the nearest-neighbor particle environment to quantify how local fluid structural fluctuations correlate with particle displacements. In particular, we examine whether the shape fluctuations in the Voronoi cells' environments about the particles in compactified granular media correlate with the direction of particle displacements, as found before by

Rahman [10] in cooled liquids. However, the nonequilibrium nature of our driven particle systems leads us to expect differences from thermalized liquids. The present work provides the first direct measurements of 3D particle trajectories during compaction, with a focus on correlations between particle motion and the local particle environment. Particle rearrangements in a column of granular materials are tracked during the course of thermal cycling, and a laser sheet scanning method is used to reconstruct the configurations of the system at the end of each cycle.

Our work is distinct from other particle tracking studies in granular systems since it focuses on environmental fluctuations about the particles and correlations in particle motion in a jammed granular material that are associated with these local environmental fluctuations. While there have been recent interesting studies of single particle dynamics in two- [11,12] and three-dimensional granular fluids [13], the determination of the evolution of Voronoi-cell volumes is much more challenging. Voronoi constructions of snapshots of jammed granular systems have recently appeared, but the Voronoi network dynamics was not studied [14,15]. Such an approach is much more difficult experimentally than simple tracer particle tracking measurements since all of the particles must be tracked in time to determine the dynamical evolution of the Voronoi-cell network.

Thermal cycling provides a method of granular compaction without exciting strong motions of particles. By thermal cycling, we mean alternately heating and cooling the material and container, with one heating and cooling cycle corresponding to one perturbation. This technique leads to exponential compaction of the material with two characteristic time scales [16] if the granular material and container have different thermal expansion coefficients. While most methods of forcing rearrangements of granular matter, such as tapping of the boundaries or air fluidization, agitate

individual particles significantly (i.e., provide particles kinetic energy relative to their neighbors), thermal cycling provides a quasistationary method of evolving the structure towards a jammed state.

Experimental setup.—The granular material used is soda-lime glass beads (diameter $D = 3 \pm 0.3$ mm), poured into a transparent polymethylpentene (PMP) cylinder of diameter 5 cm (16.6D) to a height of 19.5 ± 0.5 cm (63.3D to 66.6D, based on three different pourings). This system was used in previous thermal cycling measurements [16]. The thermal expansion coefficient for PMP is 1.17×10^{-4} K^{-1}, about 1 order of magnitude larger than that of the beads (9×10^{-6} K^{-1}) [16]. Thermal expansion of the beads is considered negligible. The beads were immersed in index-matching oil (Cargille Labs type DF [17]) which contains 2.08 μg/ml laser dye (Nile Blue 690 perchlorate). A transparent weight of 145.5 g was placed on top of the particles to monitor the filling height and to apply a controlled vertical force.

The cylinder is placed inside a transparent water tank for thermal cycling at a rate of 16 °C/hr. As the PMP container was heated (cooled), the cross-sectional area expanded (contracted) by 0.46 mm^2 for every degree heated (cooled) (6.5% of a single particle cross section).

The sample and oil are index-matched at room temperature. Since the index of refraction changes with temperature differently for glass and oil, we can only image our sample at the end of each thermal cycle.

Three-dimensional images of the system at each cycle were obtained using a laser sheet scanning method, first described in [18,19]. Briefly, a laser sheet is sent through the specimen at the excitation frequency of the laser dye to produce a cross-sectional image of the granular material in which the particles appear as dark circles within the dyed fluid (see Fig. 1). Images are taken with a high sensitivity cooled CCD camera (Sensicam, PCO). To obtain a three-dimensional image, the laser is translated in 100 μm increments along the axis of the cylinder for a distance of 60 mm (20D), starting from the top of the pile. The camera is not translated, but the changing object distance is accounted for in our analysis.
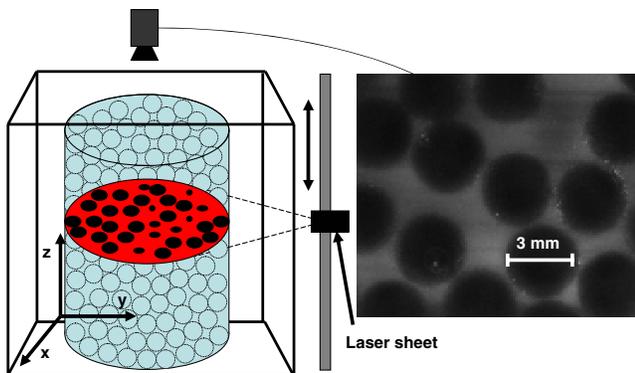
A 3D bandpass filter is used to reduce noise and to smooth out images of the beads. A particle tracking algorithm by Crocker and Grier [20] and Weeks [21] detects the centers of >98% of all beads to within 100 μm, which is smaller than the uncertainty in the bead diameters. The remaining <2% of bead positions are detected manually with comparable resolution using an interactive 3D visualization of images with an overlay of extracted particles. This allows us to generate complete maps of 3D jammed states. Particle rearrangements are followed through multiple thermal cycles. The particles move by less than 0.5D in each thermal cycle, a scale small enough to allow for reliable particle tracking.

Results.—We apply ten thermal cycles for three different temperature differentials: 25, 40, and 60 °C. The fluid becomes less transparent after 10–15 thermal cycles which prevents us from acquiring longer time sequences. The average packing fraction is determined from the vertical position of the flat glass weight on top of the pile in the 3D image, and the initial conditions are generated by letting particles settle into the oil-filled cylinder. After the particles settle, the glass top is allowed to sink onto the surface of the fluid-immersed particles. Filling in oil first is necessary to eliminate air bubbles from the sample but leads to significant variability in the initial packing fraction. Nevertheless, the increase in packing fraction during thermal cycling can be fit with an exponential $\rho(t) = \rho_0 - Ae^{-t/\tau}$ as shown in Fig. 2 using an implementation of the Levenberg-Marquardt algorithm [22]. In all cases, the compaction rate is slower than the faster of the two time scales, 2.72 cycles, reported in Ref. [16], consistent with a weaker forcing of the particles due to buoyancy forces.

We find that the pair correlation function $g(r)$, defining the average local particle density, does not evolve significantly during compaction, as shown in the inset in Fig. 3.

FIG. 1 (color online). Experimental setup: Glass beads immersed in index-matching oil in a cylinder are subjected to thermal cycling via a water bath. The fluorescently dyed fluid is imaged via a laser sheet that is moved across the sample. One of 600 cross-sectional images shown.
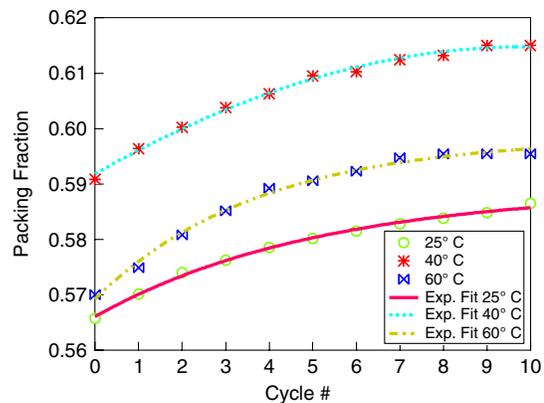
FIG. 2 (color online). Packing fraction vs cycle number for various temperature differentials. $\tau = 5.2 \pm 0.4$ cycles for $\Delta T = 25$ °C, $\tau = 4.9 \pm 0.3$ cycles for $\Delta T = 40$ °C, and $\tau = 3.8 \pm 0.3$ cycles for $\Delta T = 60$ °C.

This is not surprising since the particles need to move closer only by about $0.015D$ on average to achieve an increase in packing fraction of 1.5%. The overall shape of $g(r)$ is consistent with a random arrangement of particles in the presence of some ordering at the boundaries.

The Voronoi construction defines a unique partitioning of space where each particle is assigned a local neighborhood, the Voronoi cell, corresponding to the region of space closest to a given particle. The Voronoi-cell structures were determined using the QHULL algorithm [23]. To avoid boundary artifacts, Voronoi cells were computed for all particles, but only the volumes of particles that are not on the boundaries we used in the analysis. The distributions of Voronoi-cell volumes are shown in Fig. 3. The distribution is non-Gaussian with a sharp cutoff at small volumes and a broad range of large volumes, similar to distributions observed in simulations in glass-forming liquids [24] and in recent experiments of granular materials [15]. One possible functional form of the distribution of Voronoi-cell volumes proposed by Aste *et al.* [15] contains only one fitting parameter k. Fitting our Voronoi-cell volume distributions to this function yields $k = 14.2 \pm 0.6$, which is close to the range of k values suggested by Aste *et al.* [15]. We also find that the distribution of Aste *et al.* is consistent within numerical uncertainty with the Voronoi-cell volume distribution found in the recent molecular dynamics simulations of Starr *et al.* for a variety of cooled molecular liquids (polymeric, water, and silicon) [24]. Moreover, the Voronoi-cell volume distribution does not change significantly as the system is compacted. Our observations thus provide further evidence of the universality of the Voronoi-cell volume distribution of strongly interacting fluids.

Following Rahman's investigation of cooled liquids, we analyze particle motion and its relation to the Voronoi-cell shape. We define the vector $\vec{v}_{i,j}$ to be the displacement of the center of particle i from cycle j to $j + 1$ (see Fig. 4). Next, we define a vector describing the Voronoi-cell shape relative to the particle center. From the perspective of the
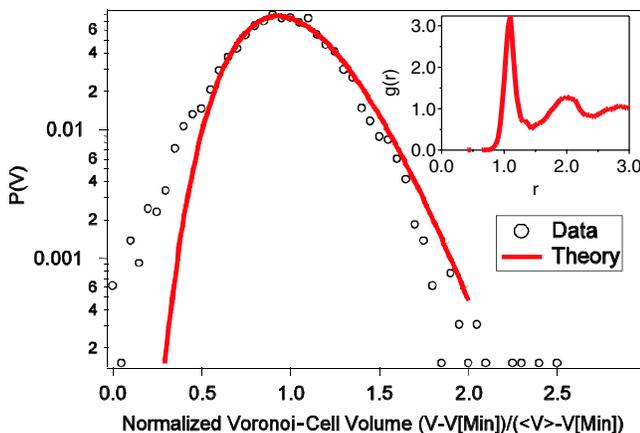
particle, the vertices of the Voronoi construction correspond to the direction in which a particle "sees" a void among three neighbors. The mean position of all vertices therefore indicates where a particle would see more local void spaces. The vector $\vec{u}_{i,j}$ defines the displacement from the center of particle i at cycle j to the mean position of its corresponding Voronoi vertices, as shown in Fig. 4. The averages for $|\vec{u}|$ and $|\vec{v}|$ are approximately 1 mm ($0.33D$) larger than the accuracy with which we detect particle positions. The magnitudes and directions of the two vectors were found to be uncorrelated to the volumes of their corresponding Voronoi cells.

To determine the correlation between particle displacement and Voronoi shapes, we then consider the alignment of $\vec{u}_{i,j}$ and $\vec{v}_{i,j}$. Specifically, we calculate $\cos(\theta)$ for each image, where θ is the angle between $\vec{u}_{i,j}$ and $\vec{v}_{i,j}$ for each particle. The probability distribution of $\cos\theta$ averaged over all cycles is shown in Fig. 5. In addition, we show the distribution for the first and the last cycles and a control for two 3D images without thermal cycling between the images. We find that the distribution peaks at $\cos\theta = 1$, indicating that the particle moves toward the center of the vertices of its Voronoi cell. Particle motion and Voronoi-cell shape are indeed correlated. This correlation was found to be independent of either the size of the Voronoi-cell volumes or the magnitudes of their corresponding displacement vectors.

Discussion.—By using the laser sheet scanning method, we visualize the internal structure and dynamics of a jammed granular material. Under quasistatic forcing via thermal cycling, flows are slow enough (less than $\approx 0.5D$ between frames), so we can observe the microscopic dynamics of this strongly interacting particle system. While the differences in local structures are too small to be observable in local distributions such as $g(r)$ or the Voronoi-cell volume distribution, the Voronoi-cell volume appears to hold important clues for the future dynamical evolution of the particles. Voronoi reconstruction indicates that particles tend to move toward the centers of Voronoi vertices as long ago observed in Rahman's pioneering simulations of particle motion in cooled liquids [10]. This correlated displacement in our granular fluid is inde-

FIG. 3 (color online). Histogram of Voronoi-cell volumes. Inset: Pair correlation function $g(r)$ averaged over 10 thermal cycles.
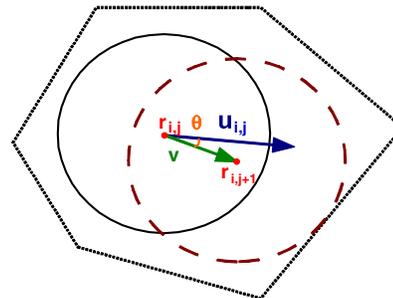
FIG. 4 (color online). Definition of particle displacement vector v and u vector for a cross section of the 3D Voronoi-cell volume.
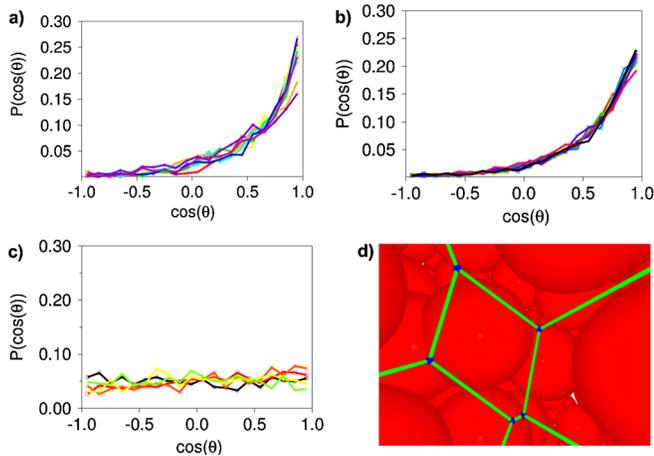
FIG. 5 (color online).   (a) Preferred direction probability distribution functions (PDFs) for a system with $\Delta T = 40\,^{\circ}\text{C}$ for each thermal cycle. (b) Preferred direction PDFs for a system with $\Delta T = 25\,^{\circ}\text{C}$ for each thermal cycle. (c) Preferred direction PDFs for a system at constant temperature. (d) 3D reconstruction of a system from the perspective of a given particle facing five vertices of its Voronoi cell. Notice that the vertex is located in the void between particles.

pendent of the size of the Voronoi-cell volume, the velocity of particles, and the position of particles within the granular column.

Rahman [10] and others [25] inferred from the correlations in the tracer particle displacement and the Voronoi-cell shape that the particles were moving in tubelike environments, thus anticipating the stringlike motion in cooled liquids that has recently become widely appreciated [8,9]. This raises questions about whether such collective interparticle displacements also characterize particle motion in compactified granular materials. The absence of equilibrium in granular fluids, however, complicates the definition of "mobile" and collectively moving particles in granular materials, since there is no model such as Brownian motion to provide a "baseline" for this comparison. Unfortunately, we cannot track particles long enough to perform a string analysis to connect the local collective dynamics with these large scale collective motions. However, a recent study of a quasi-2D air-driven granular material [5] indicates the presence of collective stringlike motion as in cooled liquids, so the general presence of such collective motions in driven granular media seems likely. The presence of such correlated motion implies the existence of correlations between shape fluctuations and particle displacements of adjacent Voronoi cells, and in future work we plan to investigate correlations between the displacement vectors describing the Voronoi-cell-shape fluctuations to better understand the origin of collective stringlike motion in strongly interacting fluids. Collective particle motion would appear as chainlike assemblies of particle displacement vectors, defining a collective coordinate for the stringlike motion.

*scsumd@umd.edu
†jack.douglas@nist.gov
‡wlosert@umd.edu

[1] C. S. O'Hern, L. E. Silbert, A. J. Liu, and S. R. Nagel, Phys. Rev. E **68**, 011306 (2003).
[2] J. B. Knight, C. G. Fandrich, C. N. Lau, H. M. Jaeger, and S. R. Nagel, Phys. Rev. E **51**, 3957 (1995).
[3] M. Toiya, J. Stambaugh, and W. Losert, Phys. Rev. Lett. **93**, 088001 (2004).
[4] A. J. Liu and S. R. Nagel, Nature (London) **396**, 21 (1998).
[5] A. S. Keys, A. R. Abate, S. C. Glotzer, and D. J. Durian, Nature Phys. **3**, 260 (2007).
[6] E. R. Weeks and D. A. Weitz, Phys. Rev. Lett. **89**, 095704 (2002).
[7] A. H. Marcus, J. Schofield, and S. A. Rice, Phys. Rev. E **60**, 5725 (1999).
[8] J. F. Douglas, J. Dudowicz, and K. F. Freed, J. Chem. Phys. **125**, 144907 (2006).
[9] C. Donati, J. F. Douglas, W. Kob, S. J. Plimpton, P. H. Poole, and S. C. Glotzer, Phys. Rev. Lett. **80**, 2338 (1998).
[10] A. Rahman, J. Chem. Phys. **45**, 2585 (1966).
[11] A. R. Abate and D. J. Durian, Phys. Rev. E **74**, 031308 (2006).
[12] O. Dauchot, G. Marty, and G. Biroli, Phys. Rev. Lett. **95**, 265701 (2005).
[13] P. Wang, C. Song, C. Briscoe, and H. A. Makse, Phys. Rev. E **77**, 061309 (2008).
[14] P. Richard, P. Philippe, F. Barbe, S. Bourlès, X. Thibault, and D. Bideau, Phys. Rev. E **68**, 020301(R) (2003).
[15] T. Aste, T. D. Matteo, M. Saadatfar, T. J. Senden, M. Schröter, and H. L. Swinney, Europhys. Lett. **79**, 24 003 (2007).
[16] K. Chen, J. Cole, C. Conger, J. Draskovic, M. Lohr, K. Klein, T. Scheidemantel, and P. Schiffer, Nature (London) **442**, 257 (2006).
[17] Identification of a commercial product is made only to facilitate reproducibility and to adequately describe procedure. In no case does it imply endorsement by NIST or imply that it is necessarily the best product for the procedure.
[18] M. Toiya, J. Hettinga, and W. Losert, Granular Matter **9**, 323 (2007).
[19] M. Toiya, Ph.D. thesis, University of Maryland, College Park, 2006.
[20] J. Crocker and D. Grier, J. Colloid Interface Sci. **179**, 298 (1996).
[21] E. Weeks, http://www.physics.emory.edu/~weeks/idl/.
[22] R. I. Shrager, J. ACM **17**, 446 (1970).
[23] C. B. Barber, D. P. Dobkin, and H. Huhdanpaa, ACM Trans. Math. Softw. **22**, 469 (1996).
[24] F. W. Starr, S. Sastry, J. F. Douglas, and S. C. Glotzer, Phys. Rev. Lett. **89**, 125501 (2002).
[25] R. Zwanzig and M. Bishop, J. Chem. Phys. **60**, 295 (1974).